



Semi-empirical models and sea level change

UNIVERSITY OF COPENHAGEN

Dina Rapp

Carlos Rodríguez

Laurent Lindpointner

supervised by
Professor Aslak GRINSTED

November 1, 2019

Contents

Chapter	Page
1 Introduction	2
2 Methods & Data	2
2.1 Background on sea level changes	2
2.2 The Model	2
2.3 Forcing required to stop SLR	3
2.4 Bayesian formulation	3
2.4.1 Reduction of Degrees of Freedom	4
2.5 Markov Chain Monte Carlo	4
2.6 Data	5
2.6.1 Sea Level Data	5
2.6.2 Forcing Data	6
3 Results	7
3.1 emcee Results	7
3.2 Check for overfitting	7
3.3 Reconstruction of the past sea level	8
3.4 Predictions of the future SLR	9
3.5 Counterfactuals	10
3.6 Anthropogenic vs. Natural Forcing	11
3.7 Forcing required to stop the sea level from rising further	11
4 Discussion	11
4.1 emcee results and variability	11
4.2 Discussion of the reconstruction of the past sea level	13
4.3 Discussion of the prediction of the future SLR	13
4.4 Counterfactuals & SLR due to anthropogenic and natural forcing	15
4.5 Importance of volcanoes	15
4.6 Forcing required to stop SLR	16
5 Conclusion	16
A emcee results table	17

1 Introduction

The purpose of this work is to follow the paper by Jevrejeva et al. [1], and use their proposed model in different scenarios. They propose a very simple model assuming a linear relationship between the equilibrium sea level and the radiative forcing, shown in equation (2). As the equilibrium sea level changes, the actual sea level changes with a time-delay described by the time-constant τ .

By using their model on recent sea level data and different forcing series past sea levels are reconstructed, future sea levels are predicted and counterfactual scenarios are investigated, to judge the influence of different components of radiative forcing on the sea level.

2 Methods & Data

2.1 Background on sea level changes

Changes in the sea level can come from either water added from other reservoirs or changes in ocean density as explained in section 6.3.2 in [2]. There is much discussion about the significance of these two drivers [1] with some holding the opinion that the main driver is density change, while others view water added by melting of sea and land ice as the dominant factor.

The changes in density are mainly caused by changes in temperature, but changes in salinity can also have a significant effect. The water added from other reservoirs comes from melting of glaciers, ice caps, ice sheets and water stored on land. All these factors would have their own characteristic response time in reality, but to simplify the system the paper by Jevrejeva et al. [1] proposes a single characteristic response time, τ , to describe all drivers.

The radiative forcing is directly related to the heat content in the ocean [3], while it is a proxy for local weather when it comes to melting of glaciers, ice caps and ice sheets and thus also a proxy for salinity changes as freshwater is added to the ocean. As there is a direct link between changes in local weather and perturbations in global radiative forcing this should be a good approximation for the simplified model used. By using this approximation it is assumed that all different drivers are described by the forcing $F(t)$.

2.2 The Model

We used the model proposed by Jevrejeva et al. in [1]. This model assumes an equilibrium sea level S_{eq} , which has a linear relationship to the radiative forcing $F(t)$:

$$S_{eq}(t) = a \cdot F(t) + b \quad (1)$$

Here, a is a sensitivity parameter of the equilibrium sea level to the forcing and b is the equilibrium sea level for forcing $F = 0$. The linearization of this relationship is valid for the Late Holocene climate [1] and therefore also for the relatively short period of time we will be looking at. The change in the sea level is given as:

$$\frac{\partial S}{\partial t} = \frac{(S_{eq}(t) - S(t))}{\tau} \quad (2)$$

where $S(t)$ is the observed sea level and τ is the characteristic response time. In this model a global response time is assumed for each of the contributing factors of sea level rise as mentioned in section 2.1. In the numerical implementation of the model, a forward Euler approach was used:

$$S(t) = S(t-1) + \frac{\partial S}{\partial t} = S(t-1) + \frac{(a \cdot F(t-1) + b) - S(t-1)}{\tau} \quad (3)$$

2.3 Forcing required to stop SLR

A visualization of the forcing required at a given point in time for the sea level to remain constant can yield interesting information when compared to the observed radiative forcing. The forcing needed to stop the sea level from rising further at a given time, is found by setting equation (2) equal to zero and replacing S_{eq} with equation (1):

$$\frac{(a \cdot F(t) + b - S(t))}{\tau} = 0 \quad (4)$$

where a is the sensitivity of the sea level equilibrium to the radiative forcing $F(t)$, b is the equilibrium sea level when there is zero radiative forcing, $S(t)$ is the sea level at the time t and τ is the characteristic response time. When equation (4) is solved for $F(t)$, τ falls away and we are left with the relationship:

$$F(t) = \frac{S(t) - b}{a} \quad (5)$$

The forcing needed to stop the SLR can be calculated with this equation.

2.4 Bayesian formulation

In the model outlined in subsection 2.2, there are 3 parameters, a, b and τ , to be tuned to fit our model to the available sea level data which poses an inverse problem. This inverse problem can be formulated in the following way, which is called Bayesian formulation:

$$P(\Theta|D) = \frac{1}{N} P(\Theta) P(D|\Theta) \quad (6)$$

where $P(\Theta|D)$ is the probability of the model given the data, $P(\Theta)$ is the prior distribution and $P(D|\Theta)$ is the likelihood function, giving the probability of the observed data given the model parameters. $1/N$ is a normalization constant.

For the emcee algorithm that was used to solve the inverse problem, the set up of the above mentioned functions was needed:

1. **model function:** modelling sea levels given forcing series
2. **logarithmic likeness function** $\log(P(D|\Theta))$: χ^2 -test to assess likeness of the model to the data using different sets of parameters
3. **prior constraints function** $\log(P(\Theta))$: limiting parameter space to physically reasonable values using prior knowledge about the parameters
4. **logarithmic probability of the model function** $\log(P(\Theta|D))$: probability of the model given the data calculated according to equation (6)

1. The model function is used as written in equation (3). It takes as arguments a set of parameters $\Theta = [a, b, \tau]$, a forcing series F and an initial sea level S_0 , being the first available sea level data point. It returns an array holding the sea level at each time-step according to equation (3). In our case that is the sea level for each year.

2. The logarithmic likeness function calls the model function for a set of parameters Θ to produce S_{model} and takes the sea level data S_{data} and its corresponding uncertainties S_{error} to calculate the likeness of the model to the data using a simple χ^2 -check:

$$L_{\text{Inlike}} = -\frac{1}{2} \frac{1}{Z} \sum_{t=0}^{t_{\max}} \left(\frac{S_{\text{data}, t} - S_{\text{model}, t}}{S_{\text{error}, t}} \right)^2 \quad (7)$$

The factor $1/Z$ is a reduction in the effective degrees of freedom because there is auto-correlation in the data. In section 2.4.1, it is described how this factor was obtained.

3. The prior constraints enforce constraints on the parameters to limit the parameter space. The probability of steps within these constraints is 1, so the prior constraints function returns $\ln(1) = 0$. The probability of steps violating the prior constraints is 0, so the prior constraints function returns $\ln(0) = -\infty$.

The prior constraints we enforced are:

- $-1 < a < 3$
- $-3 < b < 1$
- $10 < \tau < 120$

The priors were chosen this tightly for practical reasons. After running the emcee several times with very loose priors, values well within these ranges showed up consistently as best fit parameters. Since it was not possible for us to run the emcee with very large ensembles for performance reasons, we chose to restrict the parameter space more, to enable the emcee to find the best fit parameters within this smaller parameter space.

4. In the probability of the model function, the logarithmic likeness function and the prior constraints function are combined to return $\log(P(\Theta|D))$.

2.4.1 Reduction of Degrees of Freedom

Since the dataset that was used, as published by Dangendorf et al. in [4], shows a clear trend in the sea level (see figure 4), we were interested in reducing the effect of auto-correlation in our data on our results. This was done by first eliminating the trend in the data and then plotting the auto-correlation function. For step one, a linear regression of the data was performed. The result can be seen in figure 1. This regression model was then subtracted from the data to flatten the dataset.

In step two, the auto-correlation function was plotted (figure 2). The plot shows clearly, that the 13th point in the dataset has zero auto-correlation with the first one. Hence, a factor $\frac{1}{Z} = \frac{1}{13}$ was chosen and used in equation (7).

2.5 Markov Chain Monte Carlo

For solving the inverse problem, emcee, as introduced by Foreman et al. in [5], is used. The basic idea of Markov Chain Monte Carlo is exploration of the parameter space of the model. This is done by using a random walk and accepting or rejecting each step of the walk based on the steps transition probability. One walker Θ consists of the parameters of the model, which in our case is $\Theta = (a, b, \tau)$. The functions described in section 2.4 were used in the emcee algorithm. For the number of walkers and iterations, we chose $n_{\text{walkers}} = 1000$ and $n_{\text{iterations}} = 1500$. The emcee was run using the sea level and forcing dataset 1 described in section 2.6 for the years 1900-2006.

Figure 3 shows the walkers exploration of the parameter space. The distribution of walkers in the parameter space stabilizes very quickly, which justifies the use of 'only' 1500 iterations.

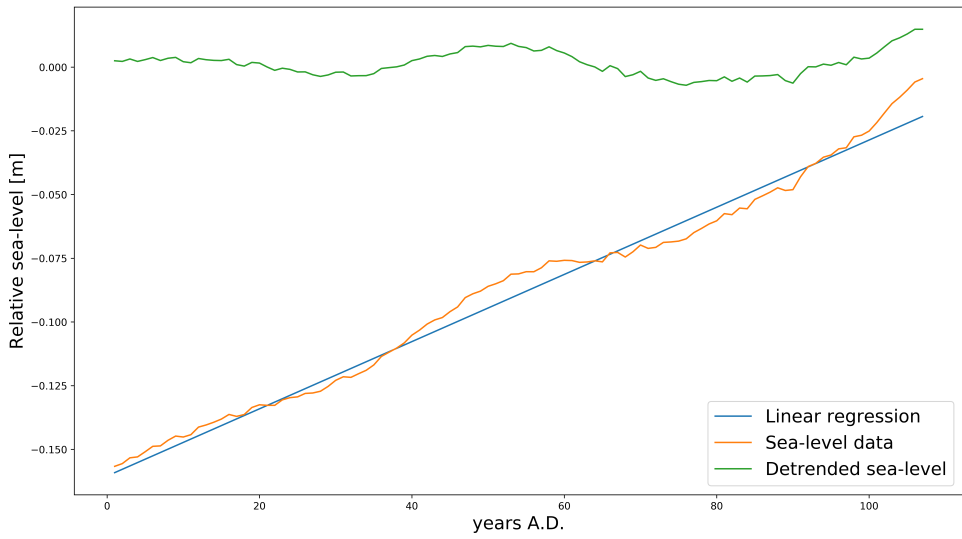


Figure 1: Linear regression performed on the sea level dataset to eliminate the trend in the data. The green curve shows the detrended dataset.

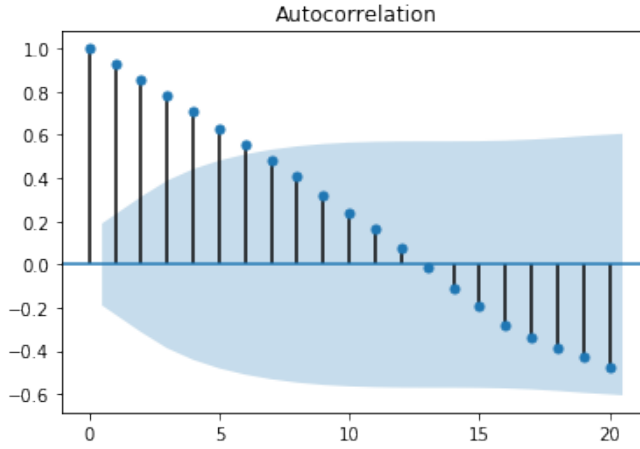


Figure 2: Auto-correlation plot for the detrended sea level dataset.

2.6 Data

2.6.1 Sea Level Data

For calibration of emcee, a dataset for sea level for the years 1900-2015 proposed by Dangendorf et al. in [4] was used. The data is given as monthly relative global mean sea level and 1 sigma error. For our purposes, we took the average sea level and sigma error for each year. Figure 4 shows the sea level data used including its 1 sigma error area.

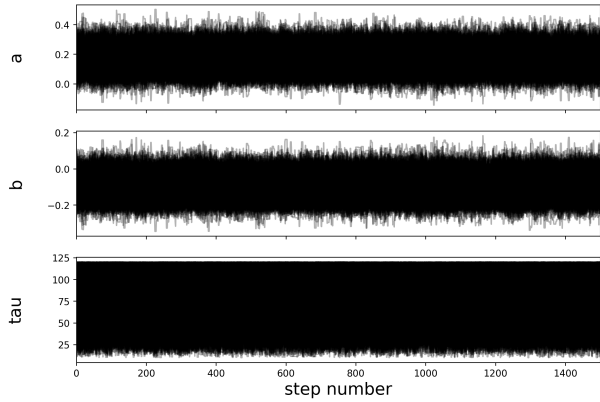


Figure 3: The walkers exploration of the parameter space. Quick stabilization of preferred range in the parameters justifies number of iterations used.

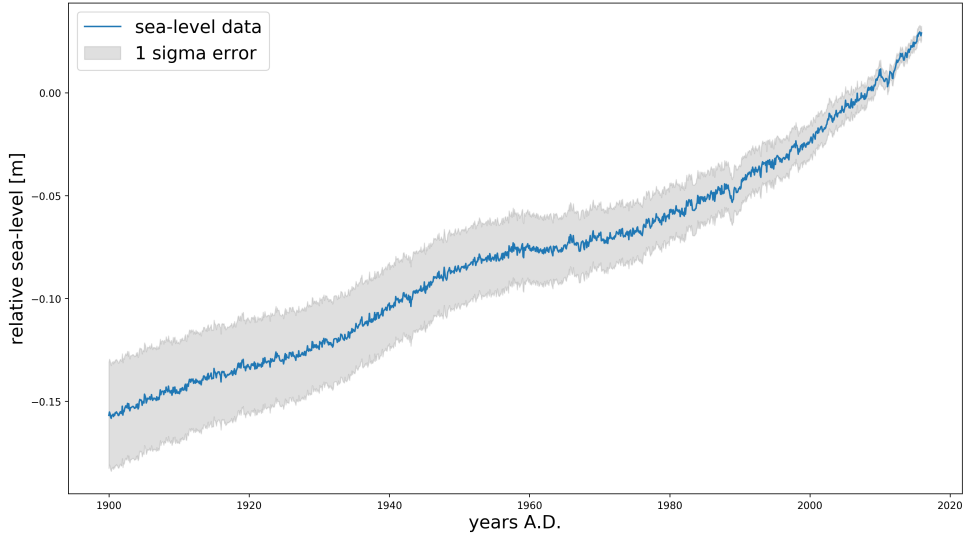


Figure 4: sea level data as proposed by Dangendorf et al. in [4] including shaded area representing the given 1 sigma error in the data.

2.6.2 Forcing Data

Forcing dataset 1: The forcing data used for calibration of the emcee was proposed by Meinshausen et al. in [6]. Data is given as total radiative forcing and forcing of individual components for the years 1765-2500. Volcanic forcing data is given up to and including the year 2006 which is why the calibration period was chosen as [1900, 2006].

Forcing dataset 2: The forcing data used for reconstruction of past sea levels was proposed by Schmidt et al. in [7]. In this data set there are 1 solar forcing data, 2 different volcanic forcing data, 6 different solar forcing data and 1 land use radiating forcing. In general, the average of the different volcanic and

solar data will be taken for the reconstruction of the past. The data is given from year 850 to year 2000, except for the land use data, it is given from year 850 to year 1992.

As at some point both datasets were needed to be together, they were glued. Both datasets have near values of the total forcing between year 1900 and year 2000. For that reason, they were glued in year 1906, jumping from dataset 1 to dataset 2. This was done instead of making the average, to have the same SLR values that they were obtained with the model in the range between year 1900 and year 2005.

3 Results

3.1 emcee Results

The parameters which deliver the best fit for our model to the data are: $a = (0.145 \pm 0.002) \text{ m}^3/\text{W}$, $b = (-0.125 \pm 0.002) \text{ m}$ and $\tau = (63 \pm 2) \text{ years}$.

Figure 5 shows the model, plotted against the data used to generate the model parameters in the emcee.

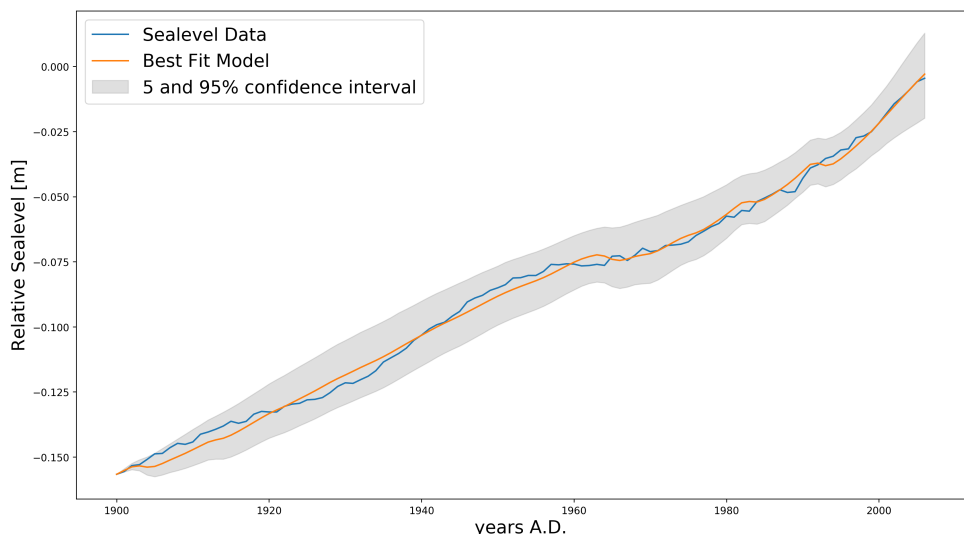


Figure 5: From forcing data set 1. Model plotted using the parameters with the maximum likeness of the model to the data from the emcee. Parameters used to generate this specific plot: [$a = 0.14565395 \text{ m}^3/\text{W}$, $b = -0.12441756 \text{ m}$, $\tau = 63.33607904 \text{ years}$]. The grey area shows the 5 and 95 % confidence interval.

3.2 Check for overfitting

Bayesian models, like most others, can be overfitted to the data used to create the model. Before the term for reduction of degrees of freedom was introduced (see section 2.4.1), the confidence interval of the fitted line in figure 5 was significantly more narrow. By reducing the degrees of freedom corresponding to the linear trend in the data we obtained the confidence interval shown in figure 5. It is assumed this is wide enough to assume the model parameters are a good fit, and not overfitted to the data used in the emcee.

3.3 Reconstruction of the past sea level

Using the result from the emcee fitting for equation (2), it is possible to model the sea levels of the past. The reconstruction of the past sea level can be done in two different ways. The first one is backwards, starting in the present and from that point calculating the sea level in the past. The second method assumes that the sea level had a certain value at some point in the past, and then calculating the sea level forward from that situation. The general problem with a backward solution of equation (2) is that it is very unstable. This can be seen in figure 6, where a change of about 15 % of the initial value generates a relatively big change in the sea level after several years.

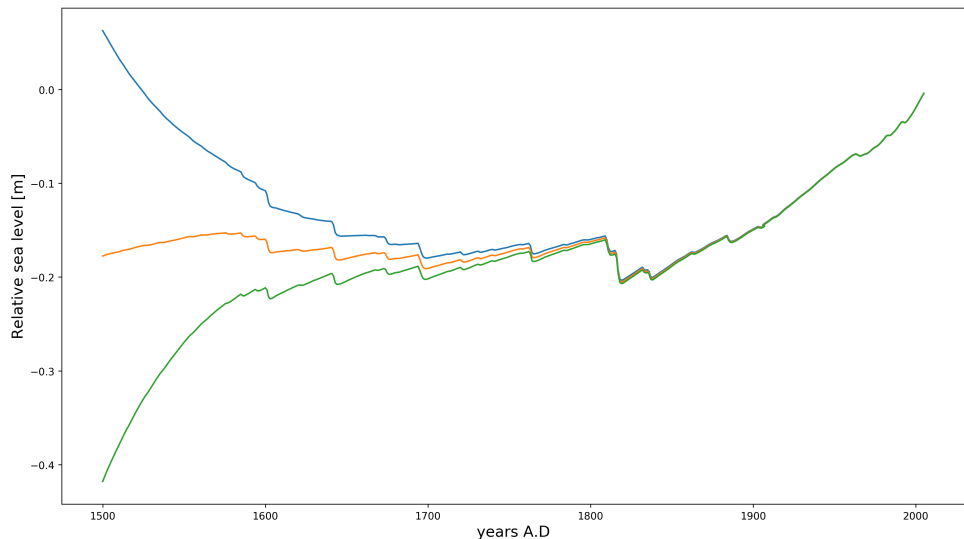


Figure 6: From forcing data set 1+2. Representation of different possible sea levels of the past for different initial values at year 1992. The blue curve corresponds to an initial value of -0.00697 , the orange curve is -0.00707 and the green curve -0.00717 .

As seen in figure 6, the three sea level curves are equal until year 1800, for a further reconstruction, they split. Hence, a forward solution of the equation (2) should be stable. This means that, an initial random value of the sea level at year 850 should not have high impact in the sea level after some years. For that reason, instead of trying to use a backward method, it is better to use a forward method for different initial values and look how many years can be trusted. The change in the sea level should not be too high without the anthropogenic forcing. In [8] it is seen that the sea level before the industrial age, between 1700 and 1850, change a range of 20 cm. Therefore, as the lowest sea level of the sea level data set is 0.156 cm, $[-0.056, -0.256]$ m is an acceptable range of values to start the simulation.

As seen in figure 7, the sea level gets stable around year 1200. From this year on, the different simulations give the same values. This means that the model used is very stable and abrupt changes in the sea level will be corrected after some years. This effect can be seen when the sea level is plotted with the forcing in figure 8. Whenever the volcanic forcing changes the sea level abruptly, the sea level gets back to its initial position after some delay.

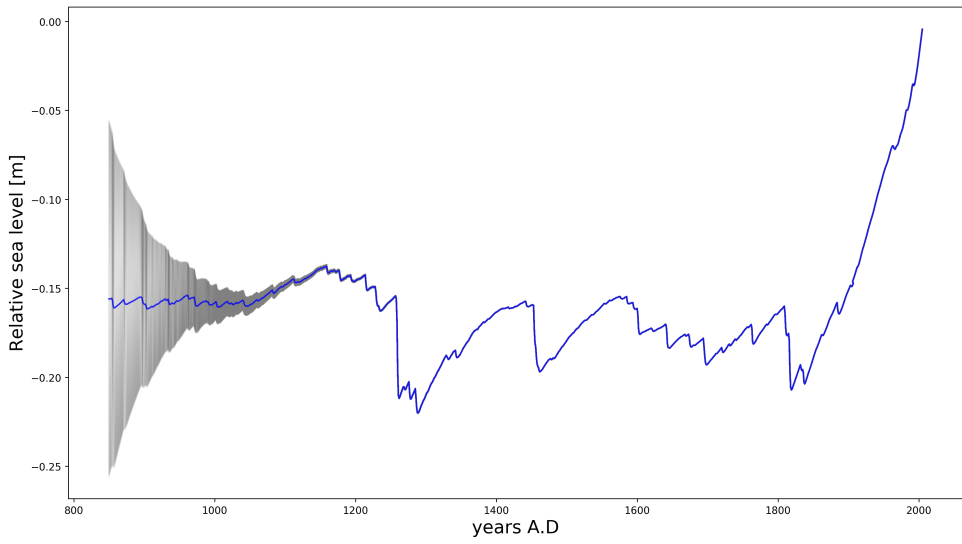


Figure 7: From forcing data set 1+2. Representation of different possible sea levels of the past for different initial values at year 800. The blue curve is with an initial sea level of -0.156 m and the grey shadow represents the interval between -0.056 m and -0.256 m.

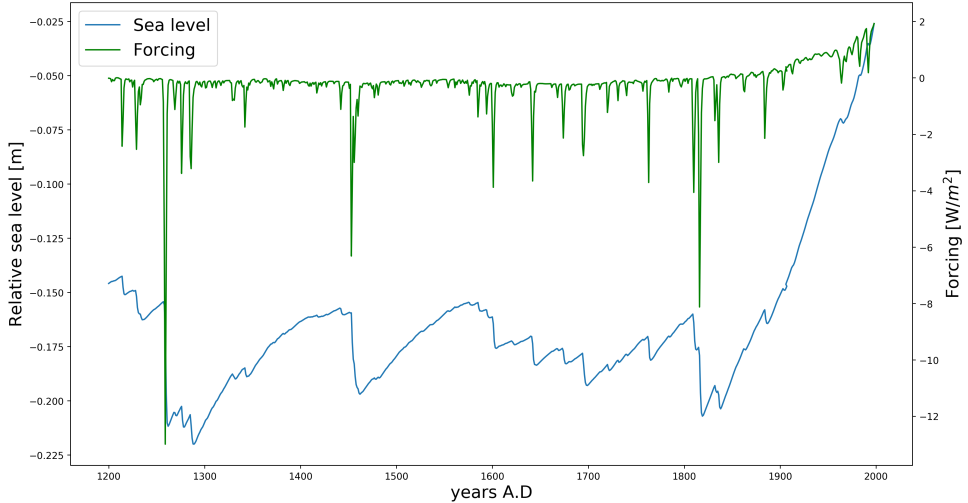


Figure 8: From forcing data set 1+2. Representation of the sea level and the forcing since 1200. The blue curve is the sea level and the green is the total forcing.

3.4 Predictions of the future SLR

Predictions for future SLR are made using the model, obtained from the emcee fitting discussed in section 3.1, and four different RCP scenarios for future radiative forcing outlined by Meinshausen et al. in [6] (figure 9).

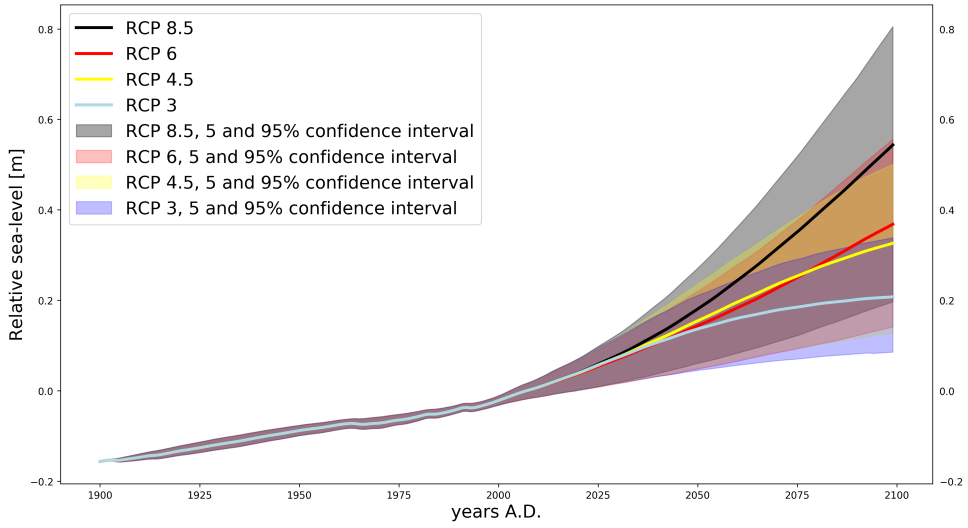


Figure 9: From forcing data set 1. Predictions for future sea levels using the parameters obtained from the emcee and four different RCP scenarios for future radiative forcing.

Table 1 shows the predicted sea levels for the years 2100 and 2500, relative to the year 2000, as well as the 5 and 95 % confidence intervals for those values.

Scenario	sea level in 2100 relative to 2000	sea level in 2500 relative to 2000
RCP 8.5	$0.56_{0.21}^{0.82}$ m	$1.68_{0.74}^{3.08}$ m
RCP 6	$0.39_{0.16}^{0.57}$ m	$0.76_{0.35}^{1.44}$ m
RCP 4.5	$0.34_{0.15}^{0.52}$ m	$0.50_{0.24}^{0.97}$ m
RCP 3	$0.23_{0.10}^{0.36}$ m	$0.08_{0.02}^{0.22}$ m

Table 1: From forcing data set 1. Sea level predictions for the years 2100 and 2500 relative to 2000 in RCP scenarios 8.5, 6, 4.5 and 3. The sea level prediction in the RCP 3 scenario peaks around 2100 and then starts declining again. The sub- and superscribed numbers show the 5 and 95 % confidence intervals of these results.

3.5 Counterfactuals

Having the different components of radiative forcing allows for running the model with or without different components and examining their influence on the resulting sea level. Figure 10 a. shows sea level reconstruction using total radiative forcing, anthropogenic forcing only as well as total radiative forcing minus the component for anthropogenic forcing. As a starting point sea level in 1765, -0.15 m relative sea level was used. This value was chosen as an approximation judging by sea level reconstruction reaching farther back. The sea level will then approach the proper equilibrium sea level according to the forcing. This process was also shown in figure 7, and hence values up to about 1850 should not be taken seriously, but regarded as a burn in phase for the reconstruction.

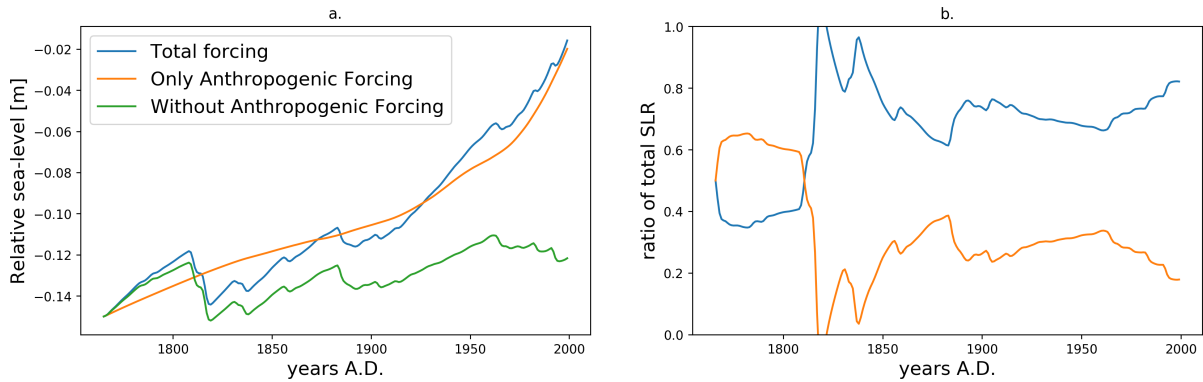


Figure 10: From forcing data set 1. a.: Modelled sea levels starting 1765 using the total past forcing, only anthropogenic forcing and forcing omitting the anthropogenic component. b.: Ratio between SLR due to anthropogenic forcing (blue curve) and SLR due to natural forcing (orange curve) since 1765.

3.6 Anthropogenic vs. Natural Forcing

Considering the SLR due to separately anthropogenic and natural forcings allows us to look at their individual influence on the development of the global sea level since 1765. Figure 10 b. shows the ratio between SLR due to anthropogenic and natural forcing.

Averaging over the proportion of SLR due to these components for the 20th century gives a ratio of 71.3 % of SLR due to anthropogenic forcing and consequently 28.7 % of SLR due to natural forcing. The sea level rose in the 20th century by a total of 13.49 cm. This means a rise of 9.62 cm due to anthropogenic forcings and a rise of 3.87 cm due to natural forcings.

The figure also shows natural forcings being the dominant driver of sea level rise prior to 1810 before an onset of strongly negative volcanic forcing in the years after. From the year 1850 onward, when the effects of volcanic activity in the early 19th century have subsided, anthropogenic forcings show to have the dominant impact on sea levels.

3.7 Forcing required to stop the sea level from rising further

By using the sea level data described in section 2.6.1 and equation (5) with the parameters given in section 3.1 from the emcee, the curve visualized below in plot 11a is obtained. Plot 11b shows the difference between the forcing dataset 1 and the calculated forcing to stop SLR. The linear trend of the difference is also plotted with its standard error. This error is so small that it barely can be seen in the plot. The magnitude is ± 0.00093 [W/m²].

4 Discussion

4.1 emcee results and variability

The results for the emcee fitting as presented in section 3.1 show a good fit of our model to the data. There is a fluctuation in the parameters a , b and τ in different runs, as is expected for a stochastic algorithm like emcee, however it is very small. The given uncertainties in the three parameters were inferred from multiple runs as shown in table A in appendix A. It shows the results for the parameters of 10 different runs with the same starting parameters (1000 walkers, 1000 iterations, initial position in

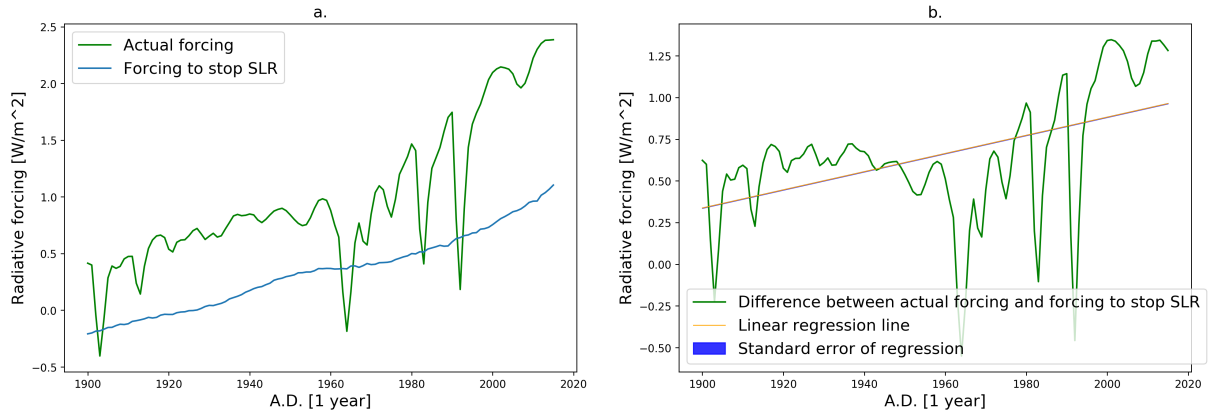


Figure 11: From forcing data set 1. a.: Observed radiative forcing (forcing dataset 1) and the radiative forcing that would be required at each year to stop the sea level from rising further. The latter is calculated from equation (5). b.: Difference between the observed radiative forcing and the radiative forcing required to stop SLR with a linear regression line to show the linear trend of the difference. The blue shaded area barely visible is the error of the regression.

parameter space [0.145, -0.124, 60]), as well as the mean squared error of the model when compared to the actual sea level data. In addition to there being very little fluctuation in the parameters, the quality of the fit remains virtually constant. This can also be seen in plot 12, which shows the models run with the 10 parameter sets shown in table A. The different curves cannot be distinguished from each other in the plot.

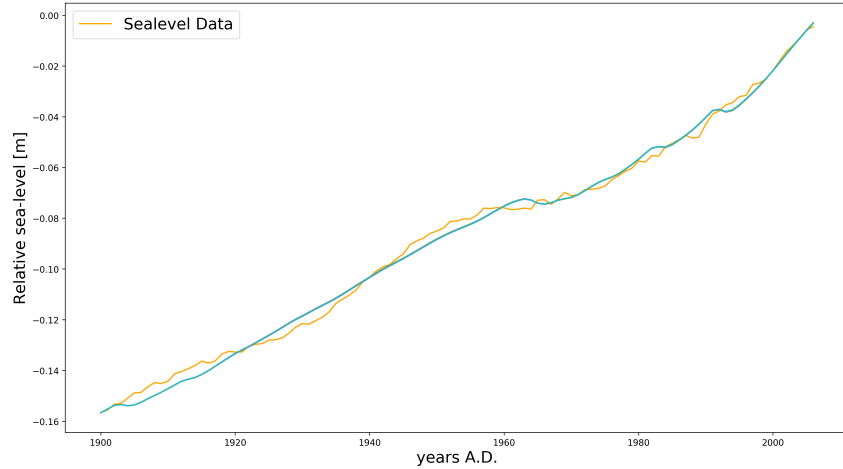


Figure 12: From forcing data set 1. Model run with best fit parameters (a , b , τ) from 10 different runs of emcee plotted against the data. There is very little fluctuation in the best fit parameters for different runs which results in overlaying curves for the 10 different parameter sets.

4.2 Discussion of the reconstruction of the past sea level

Figure 6 SLR shows that when the reconstruction of the past SLR is done backwards, then it is nearly impossible to obtain a suitable solution. The only way to obtain a good reconstruction is to make a forward modelling, using a random initial values as in figure 7. From this method one can obtained a possible model for the past sea level, when you take the part where all the curves get equal. Figure 13 depicts the reconstructed sea level since 1200, with the confidence interval, which gives an error of nearly 0.7 m.

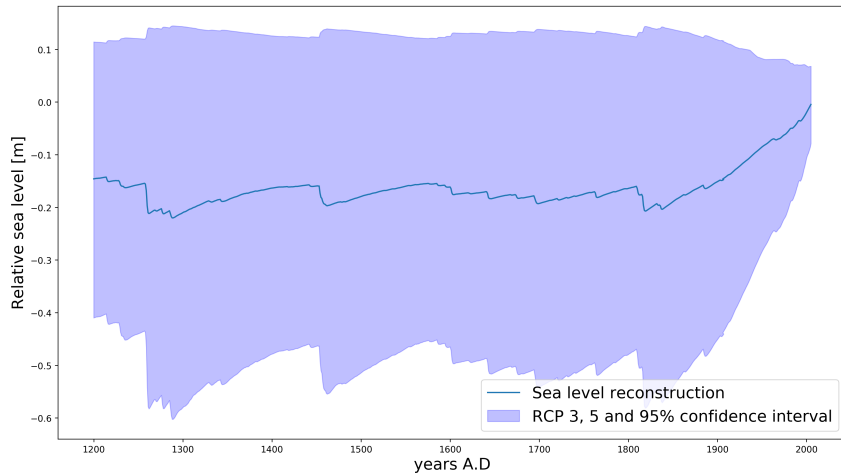


Figure 13: From forcing data set 1+2. Reconstruction of the sea level since 1200.

The reconstruction of the past sea level can be compared with [8], which gives the sea level increment between year 1700 and year 2000, 0.28 m. This value is much higher than the one seen in figure 13, which is 0.18 m in the same period.

In Figure 8 is seen that the volcanic forcing was dominant before the industrial revolution, as the most important sea level changes were made due to the stochastic volcanic forcing. This can be seen when the volcanic effects are taken out.

In Figure 14 is seen that when the volcanic forcing is erased, then, the sea level goes up, in the worst case around 10 cm. This means that without volcanic effects, the sea level in 2000 would be 2 cm higher and that before the industrial age, the volcanos helped to reduce the sea level.

4.3 Discussion of the prediction of the future SLR

In figure 9, the four different future scenarios for total radiative forcing (excluding volcanic forcing) are presented. Scenario RCP 8.5 predicts a SLR to $1.68_{0.75}^{3.03}$ meter in 2500, relative to the sea level in 2000. In scenario RCP 3 the anthropogenic forcing, and thus the sea level also, rises until about 2100, and then decreases steadily. The SLR prediction of scenario RCP 3 peak at $(0.23_{0.09}^{0.34})$ meters, and in 2500 it has decreased to slightly above zero, relative to 2000. All the predictions show an increasing sea level until 2100, where scenario RCP 3 starts to decrease, while scenarios RCP 4.5 and RCP 6 stabilize from about 2200 on at around 0.5 and 0.75 respectively. Scenario RCP 8.5 stabilizes from about 2400 on at about 1.7 meters.

Table 2 shows sea level predictions for the year 2100 of different papers. The predictions by Zickfeld et al. in [9] are purely for sea level rise due to the ocean's thermal expansion.

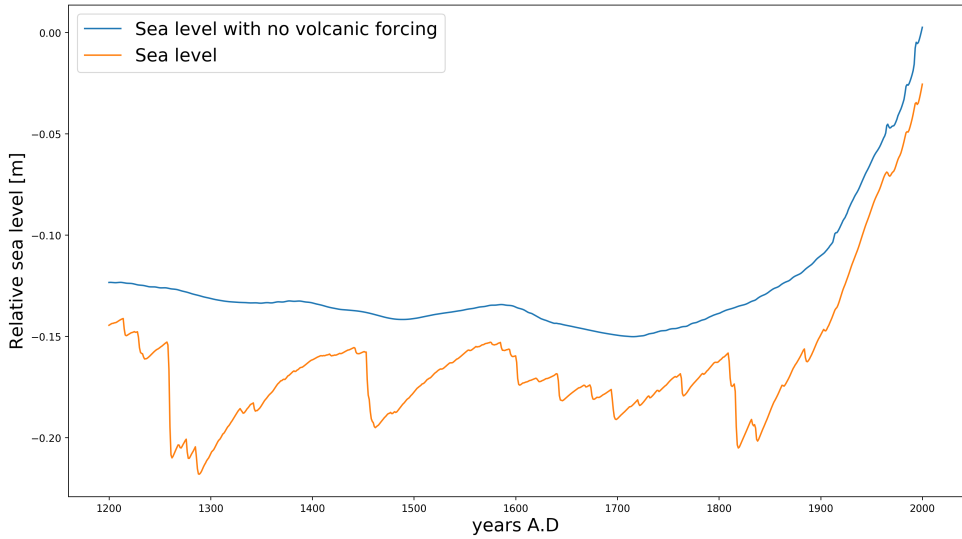


Figure 14: From forcing data set 2. Reconstruction of the sea level since 1200, with (orange) and without (blue) volcanic forcing.

	Our model	Zickfeld et al. [9]	Kopp et al. [10]	Kopp et al. [11]
RCP 8.5	$0.56_{-0.21}^{+0.82}$ m	0.3 m	$0.76_{-0.52}^{+1.31}$ m	$0.79_{-0.55}^{+1.21}$ m
RCP 6	$0.39_{-0.16}^{+0.57}$ m	0.2 m	-	-
RCP 4.5	$0.34_{-0.15}^{+0.52}$ m	0.2 m	$0.51_{-0.33}^{+0.85}$ m	$0.59_{-0.36}^{+0.93}$ m
RCP 2.6/3	$0.23_{-0.10}^{+0.36}$ m	0.15 m	$0.38_{-0.24}^{+0.61}$ m	$0.50_{-0.29}^{+0.82}$ m

Table 2: Predictions of future SLR relative to year 2000 sea level in RCP scenarios 8.5, 6, 4.5 and 3/2.6 with our model and compared to predictions by Zickfeld et al. in [9] (read from figure hence no confidence bounds given, see figure 15), Kopp et al. in [10] and [11]. The sub- and superscribed numbers indicate the boundaries of the 5 and 95 % confidence interval.

While some of our values fall narrowly into the confidence intervals of the numbers given in the two papers by Kopp et al., they are still way below theirs. There are two main reasons for that.

Firstly, it was shown by Cheng et al. in [3] that there is a direct link between radiative forcing and heat content in the ocean. Therefore, our model does well in modelling the sea level changes due to thermal expansion of the ocean. However, it does not account as well for sea level changes due to other drivers, like melting of ice. Hence, it makes sense that our predictions lie between those in figure 15, which predicts SLR due to the ocean's thermal expansion, and those in the papers by Kopp et al., which probably model the change in sea level due to other drivers better than our model.

Another reason is that the sea level data that was used to calibrate our model in the emcee shows a rise in sea level between 1900 and 2000 of 0.135 m, while the data used by Jevrejeva et al. in [1], which was proposed by Jevrejeva et al. in [8], shows a SLR of approximately 1.8 meters for that time period. Since our model fits a weaker rise in that period, this trend is continued into the future.

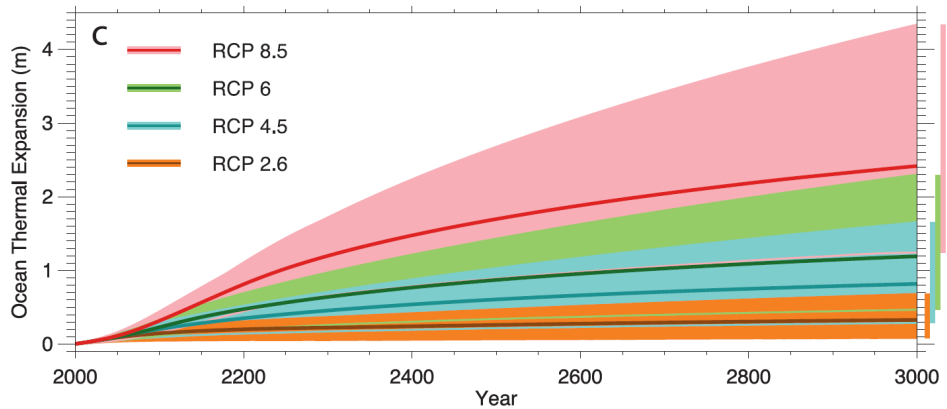


Figure 15: From [9]. Predictions for sea level rise due to thermal expansion of the ocean in four different scenarios: RCP 8.5, 6, 4.5 and 2.6.

4.4 Counterfactuals & SLR due to anthropogenic and natural forcing

Figure 10 a. shows a clear dominance of anthropogenic forcing in SLR in the 20th century. Only using the anthropogenic forcing actually yields sea levels that are almost as high as with the total forcing. This is due to negative natural forcings in multiple periods of time in 1765-2000, while the anthropogenic forcing is positive for the whole period. If there was no anthropogenic forcing since 1765, our model calculates a SLR of only about 4 cm since then. While if there was only anthropogenic forcing, our model shows almost the same SLR as with the total forcing.

Adding the sea level curves due to only anthropogenic and only natural forcings yields higher sea levels than the model run for the total forcing. However, it still allows for calculation of the ratio of total sea level rise, that is due to these two factors respectively, which is plotted in figure 10 b. The values for the ratios in SLR we get from this are close to the ones given in [1], which are 25 % of total SLR due to natural forcing and more than 70 % of SLR due to anthropogenic forcing.

4.5 Importance of volcanoes

In figure 8 there are drops in the sea level curve corresponding to volcanic eruptions (abrupt drops in the radiative forcing). The sea level recovers from these bumps over the course of a few years. As shown in figure 14, when the volcanic forcing is removed from the forcing data we have a smoother sea level curve which for this time period is higher than the one including volcanic forcing. Thus it seems the volcanic activity generally lowers the sea level as well as produce bumps right after eruptions as discussed in subsection 5.2.

This is part of the uncertainty in the RCPs, as they have a generally positive forcing from volcanoes for pre 2005, and zero after. As it is generally positive before, even though volcanic forcing is negative, means that setting the future volcanic forcing to zero is some kind of negative average.

The volcanic forcing generates several problems to simulate them. Hence, the data set from which the reconstruction of the past forcing was obtained gives two possible volcanic forcings. One with more intense volcanic activity than the other. For the general reconstruction of the past sea level, it was taken the average between both volcanic forcing data. Although, it is interesting to see how the SLR changes when both models are used.

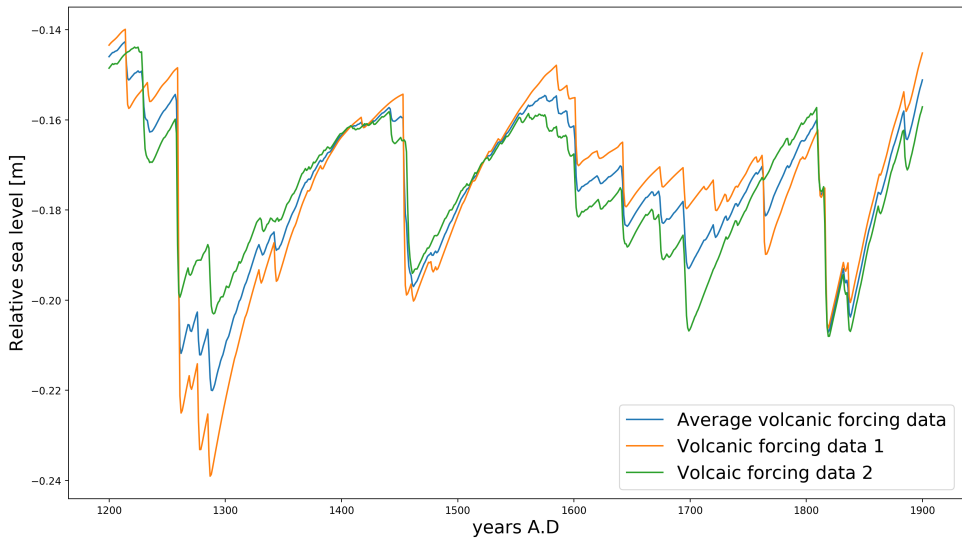


Figure 16: From forcing data set 2. Reconstruction of the sea level since year 1200, for the different reconstructions of the past volcanic forcing, in blue the average volcanic forcing, in orange the most intense volcanic forcing data and in green the less intense volcanic forcing.

Figure 16 shows the sea level for the two different volcanic data and the average between them. From it can be obtained that the average sea level difference between one or the other volcanic forcing is 0.00196 m. Also, it can be seen that the maximum difference between both curves is 0.039 m. Even if the volcanic forcing is quite difficult to simulate, with this values can be said that the uncertainty produced by this difference is 0.04 m in the sea level.

4.6 Forcing required to stop SLR

From figure 11, we see that sometimes during the drops that follow volcanic eruptions the actual radiative forcing is low enough to stop SLR. Other than this, the curve plotted in figure 11 b. showing the difference between the observed forcing and the forcing needed to stop the SLR is positive.

The difference also has a positive trend, as shown by the linear regression line plotted. If this trend continues into the future, it means that the difference between the actual forcing and the forcing required to stop SLR is increasing. This means that it will be harder and harder to lower the actual forcing to the forcing we want the larger the global radiative forcing becomes.

5 Conclusion

With the simplified model of only one characteristic response time for all the various factors driving sea level change, we can predict sea levels for the future with an acceptable confidence interval.

From the sections 4.2 and 4.3 a general difference between the past and the present can be seen. Before the industrial revolution, the volcanic forcing dominated sea level changes even with the characteristic response time counteracting the change. In the following time period, the dominating forcing is the anthropogenic forcing, accounting for about 71 % of sea level rise in the 20th century. According to RCP projections, the anthropogenic forcing, and therefore the sea level, will continue to rise in the future. As

discussed in section 4.6, it will be increasingly hard to lower the actual forcing to the forcing required to stop the sea level from rising further the larger the global radiative forcing becomes.

A emcee results table

a	b	τ	Mean squared error
0.1443927	-0.12523455	61.99732407	7.12192125e-6
0.14629474	-0.12343628	64.41716019	7.15897558e-6
0.14601088	-0.12368295	64.0576846	7.15018155e-6
0.14442935	-0.12517732	62.06164957	7.12193963e-6
0.14496879	-0.12461346	62.74428945	7.12724570e-6
0.14537135	-0.12482961	62.8282024	7.13991051e-6
0.14669732	-0.1239245	64.35129555	7.18327078e-6
0.14523953	-0.12533023	62.39698852	7.14265198e-6
0.14539989	-0.12456726	63.08348673	7.13910430e-6
0.14602055	-0.12331855	64.39164791	7.15061958e-6

Table 3: Best fit parameters obtained in emcee in 10 different runs with the same starting parameters (1000 walkers, 1000 iterations, initial position in parameter space [0.145, -0.124, 60]), as well as the mean squared error of the model when compared to the actual sea level data.

References

- [1] Svetlana Jevrejeva, Aslak Grinsted, and JC Moore. Anthropogenic forcing dominates sea level rise since 1850. *Geophysical Research Letters*, 36(20), 2009.
- [2] Hugues Goosse. *Climate system dynamics and modeling*. Cambridge University Press, 2015.
- [3] Lijing Cheng, Kevin E. Trenberth, John Fasullo, Tim Boyer, John Abraham, and Jiang Zhu. Improved estimates of ocean heat content from 1960 to 2015. *3*(3), 2017.
- [4] Sönke Dangendorf, Carling Hay, Francisco Mir Calafat, Marta Marcos, Christopher G Piecuch, Kevin Berk, and Jürgen Jensen. Persistent acceleration in global sea-level rise since the 1960s. *Nature Climate Change*, 9(9):705–710, 2019.
- [5] Daniel Foreman-Mackey, David W Hogg, Dustin Lang, and Jonathan Goodman. emcee: the mcmc hammer. *Publications of the Astronomical Society of the Pacific*, 125(925):306, 2013.
- [6] Malte Meinshausen, Steven J Smith, K Calvin, John S Daniel, MLT Kainuma, Jean-Francois Lamarque, Km Matsumoto, SA Montzka, SCB Raper, K Riahi, et al. The rcp greenhouse gas concentrations and their extensions from 1765 to 2300. *Climatic change*, 109(1-2):213, 2011.
- [7] G. A Schmidt. Enhancing the relevance of palaeoclimate model/data comparisons for assessments of future climate change. *J. Quat. Sci.*, 25:79–87, 2010.
- [8] Svetlana Jevrejeva, JC Moore, A Grinsted, and PL Woodworth. Recent global sea level acceleration started over 200 years ago? *Geophysical Research Letters*, 35(8), 2008.
- [9] Kirsten Zickfeld, Michael Eby, Andrew J. Weaver, Kaitlin Alexander, Elisabeth Crespin, Neil R. Edwards, Alexey V. Eliseev, Georg Feulner, Thierry Fichefet, Chris E. Forest, Pierre Friedlingstein, Hugues Goosse, Philip B. Holden, Fortunat Joos, Michio Kawamiya, David Kicklighter, Hendrik Kienert, Katsumi Matsumoto, Igor I. Mokhov, Erwan Monier, Steffen M. Olsen, Jens O. P. Pedersen, Mahe Perrette, Gwenaëlle Philippon-Berthier, Andy Ridgwell, Adam Schlosser, Thomas Schneider Von Deimling, Gary Shaffer, Andrei Sokolov, Renato Spahni, Marco Steinacher, Kaoru Tachiiri, Kathy S. Tokos, Masakazu Yoshimori, Ning Zeng, and Fang Zhao. Long-term climate change commitment and reversibility: An emic intercomparison. *Journal of Climate*, 26(16):5782–5809, 2013.
- [10] Robert E. Kopp, Andrew C. Kemp, Klaus Bittermann, Benjamin P. Horton, Jeffrey P. Donnelly, W. Roland Gehrels, Carling C. Hay, Jerry X. Mitrovica, Eric D. Morrow, and Stefan Rahmstorf. Temperature-driven global sea-level variability in the common era. *Proceedings of the National Academy of Sciences*, 113(11):E1434–E1441, 2016.
- [11] Robert E Kopp, Radley M Horton, Christopher M Little, Jerry X Mitrovica, Michael Oppenheimer, DJ Rasmussen, Benjamin H Strauss, and Claudia Tebaldi. Probabilistic 21st and 22nd century sea-level projections at a global network of tide-gauge sites. *Earth's future*, 2(8):383–406, 2014.